Free Radical Research, October 2007; 41(10): 1099–1108

informa
healthcare

Critical roles of reactive oxygen species in mitochondrial permeability transition in mediating evodiamine-induced human melanoma A375-S2 cell apoptosis

JIA YANG[1,2], LI-JUN WU[2], SHIN-ICHI TASHINO[3], SATOCHI ONODERA[3], & TAKASHI IKEJIMA[1]

[1]*China–Japan Research Institute of Medical and Pharmaceutical Sciences, Shenyang Pharmaceutical University, Shenyang 110016, P.R. China,* [2]*Department of Phytochemistry, Shenyang Pharmaceutical University, Shenyang 110016, P.R. China, and* [3]*Department of Clinical and Biomedical Sciences, Showa Pharmaceutical University, Tokyo 194-8543, Japan*

Accepted by Dr J. Keller

(Received 20 April 2007; in revised form 7 June 2007)

Abstract

Previous studies have shown that evodiamine could trigger apoptosis in human malignant melanoma A375-S2 cells within 24 h. To further investigate the biochemical basis of this activity, the roles of reactive oxygen species (ROS) and mitochondrial permeability transition (MPT) were evaluated. Exposure to evodiamine led to a rapid increase in intracellular ROS followed by an onset of mitochondrial depolarization. ROS scavenger rescued the $\Delta\Psi m$ dissipation and cell death induced by evodiamine, whilst MPT inhibitor blocked the second-time ROS formation as well as cell death. Expressions of key proteins in Fas- and mitochondria-mediated pathways were furthermore examined. Both pathways were activated and regulated by ROS and MPT and were converged to a final common pathway involving the activation of caspase-3. These data suggested that a phenomenon termed ROS-induced ROS release (RIRR) was involved in evodiamine-treated A375-S2 cells and greatly contributed to the apoptotic process through both extrinsic and intrinsic pathways.

Keywords: *Reactive oxygen species (ROS), mitochondrial permeability transition (MPT), evodiamine, apoptosis, ROS-induced ROS release (RIRR)*

Introduction

Apoptosis is the programmed process utilized by metazoans to eliminate redundant or potentially deleterious cells. Morphologic characteristics of apoptosis include cell membrane blebbing, cell shrinkage, chromatin condensation and nucleosomal fragmentation [1,2]. Apoptosis induction is arguably the most potent defense against cancer, making it a desirable end point for cancer therapy. At least two principal pathways for apoptosis have been described: one requires the activation of cell surface receptors such as Fas (APO-1/CD95), whilst the other directly targets mitochondria [3,4]. Both pathways subsequently activate proteolytic enzymes called caspases including caspase-8 or caspase-9 and then unite in the effector casapse-3 that mediates the rapid dismantling of cellular organelles and architecture [5].

The involvement of ROS in induction of apoptosis of various cancer cells has been widely reported [6–8]. Often, the ability of a therapeutic agent to induce apoptosis of cancer cells depends upon the ability of cancer cells to generate ROS [9]. ROS including hydroxyl radicals, superoxide anions, singlet oxygen and hydrogen peroxide, are generated as by-products

Correspondence: T. Ikejima, China–Japan Research Institute of Medical and Pharmaceutical Sciences, Shenyang Pharmaceutical University, 103 Wenhua Road, Shenyang 110016, Liaoning Province, China. Tel/Fax: 86 24 23844463. E-mail: ikejimat@vip.sina.com

ISSN 1071-5762 print/ISSN 1029-2470 online
DOI: 10.1080/10715760701499356

of cellular metabolism, primarily in the mitochondria. Cellular antioxidant systems including antioxidant molecules such as glutathione (GSH) and antioxidant enzymes such as superoxide dismutase (SOD) act in concert to detoxify these species. When the balance is disrupted, a condition referred to as oxidative stress occurs. If oxidative stress persists, oxidative damage to critical biomolecules accumulates and eventually results in several biological effects ranging from alterations in signal transduction and gene expression to mitogenesis, transformation, mutagenesis and cell death [10–12].

The mitochondrial permeability transition (MPT) pore, as described nearly 28 years ago by Haworth and Hunter [13], is an assembly of pre-existing proteins of the inner and outer mitochondrial membranes into a large conductance channel permeable to solutes of <1500 Da. Although debate still surrounds the composition of the MPT pore, it is widely considered that the MPT pore is composed of the voltage dependent anion channel (VDAC), located in the outer mitochondrial membrane, the adenine nucleotide translocase (ANT), located in the inner mitochondrial membrane (IMM), and cyclophilin D in the mitochondrial matrix [14]. MPT can result in a loss in mitochondrial membrane potential ($\Delta\Psi m$), mitochondrial swelling and rupture of the outer membrane [15].

Evodiamine (Figure 1), a bioactive component isolated from the dried, unripe fruit of *Evodia rutaecarpa* (*Goshuyu* in Japanese), was found to present catecholamine secretory, vasorelaxant, bronchial contractive, thermoregulatory, anti-nociceptive and anti-tumour effects [16–21]. Our previous study showed that evodiamine could induce A375-S2 cell apoptosis within 24 h of incubation [22]. This study was conducted to determine whether ROS and MPT were involved in the regulation of apoptotic pathways in evodiamine-treated A375-S2 cells. ROS scavengers *N*-acetyl-cysteine (NAC) and SOD as well as MPT inhibitor cyclosporine A (CsA) were used to inhibit the potential roles of ROS and MPT. $\Delta\Psi m$ and ROS levels in the treated cells were detected by specific fluorescence probes. Key proteins in regulation of mitochondria- and Fas-mediated pathway were further analysed after evodiamine administration with or without ROS scavenger or MPT blocker in A375-S2 cells.

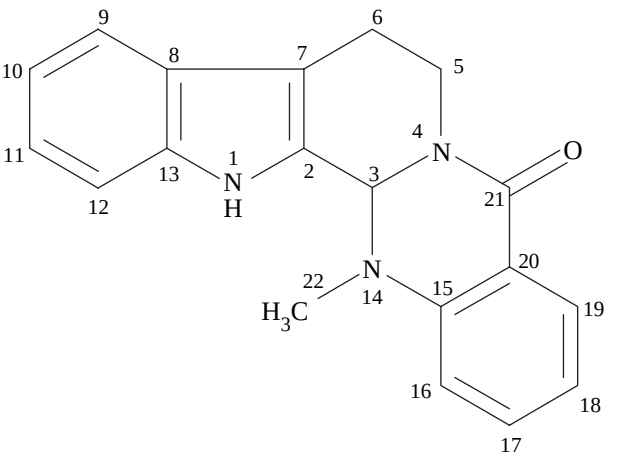

Figure 1. Chemical structure of evodiamine.

Materials and methods

Reagents

Evodiamine was obtained from Beijing Institute of Biological Products (Beijing, China); and its purity was determined to be $\sim$ 98% by HPLC measurement. Evodiamine was dissolved in dimethyl sulphoxide (DMSO) to make a stock solution and diluted by RPMI-1640 (Gibco, Grand Island, NY) before the experiments. DMSO concentration in all cell cultures was kept below 0.001%, which had no detectable effect on cell growth or death. 3-(4,5-dimetrylthiazol-2-yl)-2,5-diphenyltetrazolium bromide (MTT), 3,3-diaminobenzidine tetrahydrochloride (DAB), *N*-acetyl-cysteine (NAC), acridine orange (AO), 2′,7′-dichlorofluorescein diacetate (DCF-DA) and rhodamine-123 were purchased from Sigma Chemical (St. Louis, MO). Cyclosporin A (CsA) and superoxide dismutase (SOD) were obtained from Calbiochem (La Jalla, CA). Rabbit polyclonal antibodies against Bax, Bcl-2, SIRT1, caspase-3, Fas-associating protein with death domain (FADD), caspase-8, mouse polyclonal antibody against cytochrome *c* and horseradish peroxidase-conjugated secondary antibodies were obtained from Santa Cruz Biotechnology (Santa Cruz, CA).

Cell culture

A375-S2, human melanoma cells, were obtained from American Type Culture Collection (ATCC, #CRL, 1872, Manassas, VA) and were cultured in RPMI-1640 medium supplemented with 10% heat inactivated (56°C, 30 min) foetal calf serum (Beijing Yuanheng Shengma Research Institution of Biotechnology, Beijing, China), 2 mm L-glutamine (Gibco, Grand Island, NY), 100 kU/L penicillin and 100 g/L streptomycin (Gibco) at 37°C in 5% CO_2. Cells in the exponential phase of growth were used in the experiments.

Cytotoxicity assay

A375-S2 cells were dispensed in 96-well flat bottom microtiter plates (NUNC, Roskilde, Denmark) at a density of 5×10^4 cells/ml. After 12 h incubation, they were treated with or without NAC, SOD or CsA at given concentrations 1 h prior to the administration of 15 μm evodiamine for the indicated time periods. The cytotoxic effect was measured using the MTT assay as described elsewhere [23] with a plate reader (Bio-Rad, Hercules, CA).

The percentage of cell growth inhibition was calculated as follows:

$$\text{Cell growth inhibition (\%)} = \frac{(\text{A490, control} - \text{A490, sample})}{(\text{A490, control} - \text{A490, blank})} \times 100$$

LDH activity-based cytotoxicity assay

LDH (lactate dehydrogenase) activity was assessed using a standardized kinetic determination kit (Zhongsheng LDH kit, Beijing, China). LDH activity was measured in both floating dead cells and viable adherent cells [24]. The floating cells were collected from culture medium by centrifugation (240 × g) at 4°C for 5 min and the LDH content from the pellets was used as an index of apoptotic cell death (LDHp). The LDH released in the culture medium (extracellular LDH or LDHe) was used as an index of necrotic death and the LDH present in the adherent viable cells as intracellular LDH (LDHi). The percentage of apoptotic and necrotic cell death was calculated as follows:

$$\text{Apoptosis\%} = \text{LDHp}/(\text{LDHp} + \text{LDHi} + \text{LDHe}) \times 100$$

$$\text{Necrosis\%} = \text{LDHe}/(\text{LDHp} + \text{LDHi} + \text{LDHe}) \times 100$$

Observation of morphologic changes

The A375-S2 cells were divided into two groups and placed on culture plates for 24 h incubation. One group was treated with the control medium, the other group was treated with 15 μM evodiamine and the cellular morphology was observed using phase contrast microscopy (Leica, Wetzlar, Germany).

Nuclear damage observed by acridine orange (AO) staining

The changes in nuclear morphology of apoptotic cells were investigated by labelling cells with the fluorescent, selective DNA and RNA-binding dye AO and examining them under fluorescent microscopy (Green fluorescence for DNA, red fluorescence for RNA) [25]. After being treated with or without 15 μM evodiamine for 24 h, the cells were stained with 20 μg/ml AO (Sigma) for 15 min and then the nuclear morphology was observed under fluorescence microscopy (Olympus, Tokyo).

Measurement of mitochondrial membrane potential

Mitochondrial membrane potential was measured by the incorporation of a cationic fluorescent dye rhodamine 123 as described [26]. After incubation with 15 μM evodiamine for the indicated time periods, the cells were stained with 1 μg/ml rhodamine 123 and incubated for 15 min at 37°C. The fluorescence intensity of cells *in situ* was observed under fluorescence microscopy. Quantitative assay was performed by a similar staining procedure as above. After treatment with evodiamine, the cells were instead collected and suspended in 1 ml PBS containing 1 μg/ml rhodamine 123 and incubated for 15 min at 37°C. The fluorescence intensity of cells was analysed within 15 min by a FACScan flowcytometry (Becton Dickinson, Franklin Lakes, NJ).

Measurement of intracellular ROS generation

After treatment with 15 μM evodiamine for the indicated time periods, the cells were incubated with 10 μM 2′,7′-dichlorofluorescein diacetate (DCF-DA) for 15 min at 37°C to assess ROS-mediated oxidation of DCF-DA to the fluorescent compound 2′,7′-dichlorofluorescein (DCF). Then cells were harvested and the pellets were suspended in 1 ml PBS. Samples were analysed at an excitation wavelength of 480 nm and an emission wavelength of 525 nm by FACScan flowcytometry (Becton Dickinson, Franklin Lakes, NJ) [27].

Western blot analysis

A375-S2 cells were treated with 15 μM evodiamine for 0, 6, 12, and 24 h or co-incubated with the given inhibitors for 24 h. Both adherent and floating cells were collected and then Western blot analysis was carried out as previously described [28] with some modification. Briefly, the cell pellets were resuspended in lysis buffer, including 50 mM Hepes (pH 7.4), 1% Triton–X 100, 2 mM sodium orthovanadate, 100 mM sodium fluoride, 1 mM edetic acid, 1 mM PMSF (Sigma), 10 μg/mL aprotinin (Sigma), 10 μg/mL leupeptin (Sigma) and lysed on ice for 60 min. After centrifugation of the cell suspension at 13 000 × g for 15 min, the protein content of supernatant was determined by Bio-Rad protein assay reagent (Bio-Rad). The protein lysates were separated by electrophoresis in 12% SDS-polyacrylamide gel electrophoresis and blotted onto nitrocellulose membrane (Amersham Biosciences, Piscataway, NJ). Proteins were detected using polyclonal antibody and visualized using anti-rabbit, anti-mouse or anti-goat IgG conjugated with horseradish peroxidase (HRP) and 3,3-diaminobenzidine tetrahydrochloride (DAB) as the substrate of HRP.

Preparation of mitochondrial and cytosolic extracts

The tested cell groups were collected by centrifugation at 200 × g at 4°C for 5 min and then washed twice with ice-cold PBS. The cell pellets were resuspended in ice-cold homogenizing buffer, including 250 nM sucrose, 20 mM HEPES, 10 mM KCl, 1 mM EDTA, 1 mM EGTA, 1.5 mM $MgCl_2$, 1 mM DTT, 1 mM PMSF, 1 μg/mL aprotinin and 1 μg/mL

leupeptin. After homogenization (40 strokes), the homogenates were centrifuged at 4200 × g at 4°C for 30 min. The supernatant was used as the cytosol fraction and the pellet was resolved in lysis buffer as the membrane fraction [29].

Statistical analysis

The results are presented as Mean ± SD. Significant changes were assessed using Student's *t*-test for unpaired data, and p-values < 0.05 were considered statistically significant.

Results

Evodiamine induced inhibition of A375-S2 cell growth

Evodiamine inhibited A375-S2 cell growth in a concentration- and time-dependent manner. Evodiamine from 3–48 μM exerted a potent cytotoxic effect on A375-S2 cell growth and treatment with 15 μM evodiamine for 24 h resulted in almost 50% inhibition (Figure 2A).

To characterize the evodiamine-induced A375-S2 cell growth inhibition, we observed the morphologic changes in the cells. When the cells were cultured with 15 μm evodiamine for 24 h, marked apoptotic morphologic alterations including membrane blebbing and nuclear condensation were observed (Figure 2D). In addition, morphologic changes were further confirmed by AO staining. In the control group, the nuclei in which DNA resides were round and homogeneously stained (Figure 2C), whereas the evodiamine-treated cells showed marked fragmented DNA in nuclei (Figure 2E). These suggested that evodiamine could induce apoptotic cell death in A375-S2 cells.

Inhibition of ROS rescued the loss of ΔΨm in evodiamine-treated cells

Since the disruption of the mitochondrial membrane potential is a critical step occurring in cells undergoing apoptosis, we evaluated whether treatment with evodiamine had any effect on ΔΨm. The integrity of mitochondrial membranes of the cells was examined by rhodamine 123 staining. The decrease in rhodamine 123 fluorescence intensity reflected the loss of ΔΨm. The fluorescent intensity of evodiamine-treated cells for the indicated time periods was observed under a fluorescence microscope or analysed by FACScan. The cells incubated with evodiamine observed a weak green fluorescence (Figure 3C) compared with bright green fluorescence (Figure 3A) in untreated cells. The quantitative analysis revealed that exposure of A375-S2 cells to evodiamine decreased the fluorescent intensity of rhodamine 123 staining from 99.05% in untreated cells to 56.23% in 24 h-treated cells (Figure 3I), representing a fall in ΔΨm before 24 h.

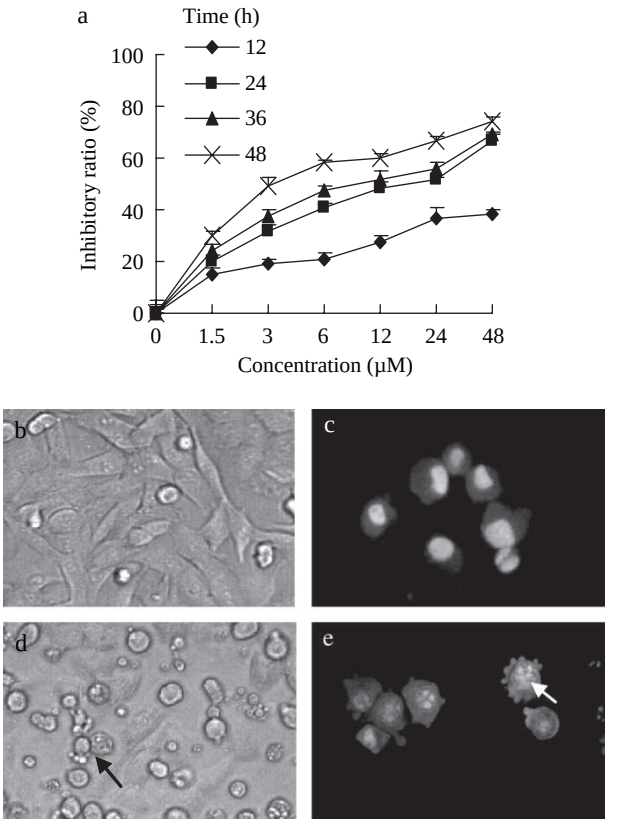

Figure 2. Evodiamine induces growth inhibition. The cells were treated with various doses of evodiamine for 12, 24, 36 or 48 h. The inhibitory ratio was measured by MTT assay (A). $n = 3$, Mean ± SD. The cellular morphologic changes were observed after the cells were incubated with medium or 15 μM evodiamine for 24 h under a phase contrast microscope (B, medium; D, evodiamine; arrow indicates multiblebbing cell; ×200 magnification) or under a fluorescence microscope by AO staining (C, medium; E, evodiamine; arrow indicates fragmented nuclear DNA; ×200 magnification).

It has been reported that ROS generation could lead to mitochondrial damage and membrane depolarization [30]. To evaluate whether ROS participated in the ΔΨm regulation, ROS scavenger NAC was introduced to dismiss the effect of ROS. Results showed that co-incubation with NAC notably reversed the dissipation in ΔΨm as illustrated by the increased number of rhodamine positive cells from 56.23% for evodiamine alone to 89.97% in the presence of NAC at 24 h (Figure 3I). These observations indicated that the collapse of ΔΨm took place after 6 h incubation with evodiamine and was mainly caused by ROS production.

Inhibition of MPT blocked the second-time ROS generation in evodiamine-treated cells

To further confirm that ROS was stimulated in evodiamine-treated cells, we measured intracellular ROS level by using the ROS-detecting fluorescent dye DCF-DA. A375-S2 cells were exposed to 15 μM evodiamine for the indicated time periods. Significant

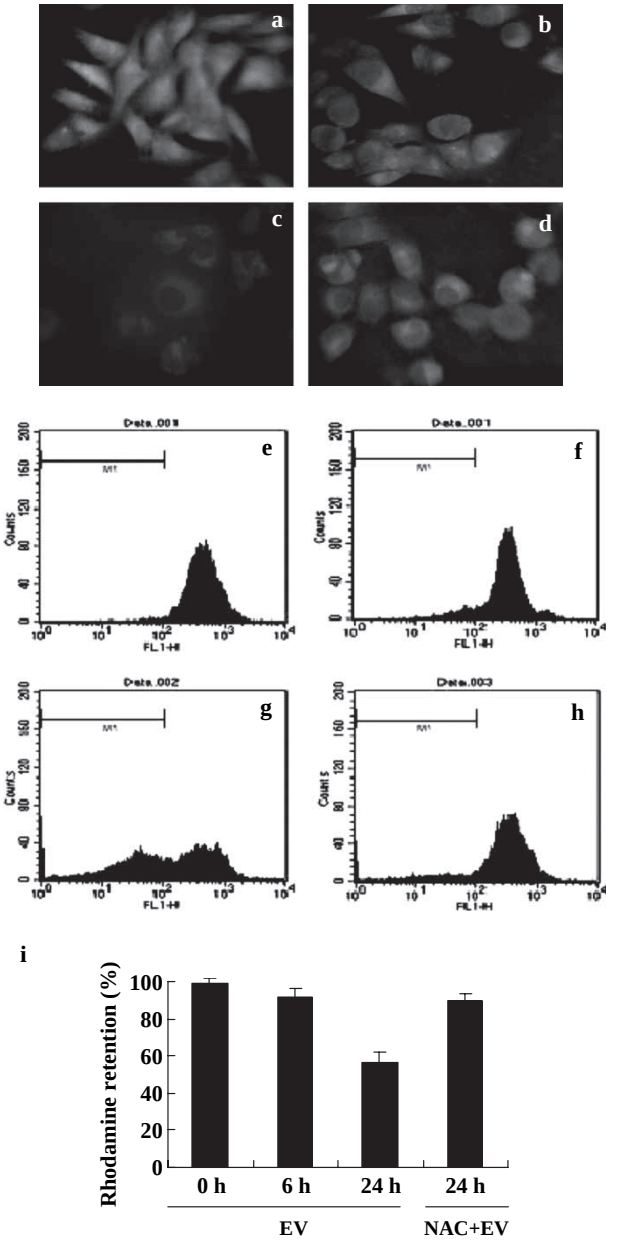

Figure 3. Significant drop in mitochondrial membrane potential ($\Delta\Psi m$) was induced by evodiamine and was rescued by NAC in A375-S2 cells. The cells were incubated with 15 μM evodiamine for 0, 6, 24 h or coincubated with 15 μM evodiamine and 1 mM NAC for 24 h. Then cells were loaded with membrane-sensitive probe rhodamine-123 1 μg/ml at 37°C for 30 min, washed and observed using fluorescence microscopy or measured by a FACScan flow cytometery after collection. The fluorescent images of treated cells are shown (A: 0 h for EV; B: 6 h for EV; C: 24 h for EV; D: 24 h for NAC+EV). The FACS histograms of treated cells are presented (E: 0 h for EV; F: 6 h for EV; G: 24 h for EV; H: 24 h for NAC+EV). The corresponding linear diagram of the FACScan histograms is expressed in (I). Data represents the rhodamine-123 fluorescence intensity displaying a decreased $\Delta\Psi m$. The values shown are mean±standard errors ($n=3$ of individual experiments).

generation of ROS was observed initially at 6 h after evodiamine treatment evidenced by enhancement of DCF fluorescence. The ratio of DCF positive cells was increased from 4.97% in untreated cells to 43.21% in 6 h-treated and 85.21% in 24 h-treated cells, respectively (Figure 4E).

Activation of MPT was proposed to contribute to the generation of ROS [31]. To clarify the role of MPT in ROS production, CsA, a MPT blocker which blocks the formation of the MPT pore by interacting with cyclophilin D from the mitochondrial matrix and preventing its joining the pore was administered. The result showed that CsA could significantly suppress the later ROS production from 85.21% to 55.77% at 24 h (Figure 4E). Thus, induction of MPT might be involved in the intracellular ROS production triggered by evodiamine in A375-S2 cells.

Inhibition of ROS or MPT alleviated cell death in evodiamine-treated cells

As the above results indicated that ROS and MPT were both induced during evodiamine incubation, we speculated the lethal roles of them in evodiamine-treated cells. ROS non-enzymatic scavenger NAC

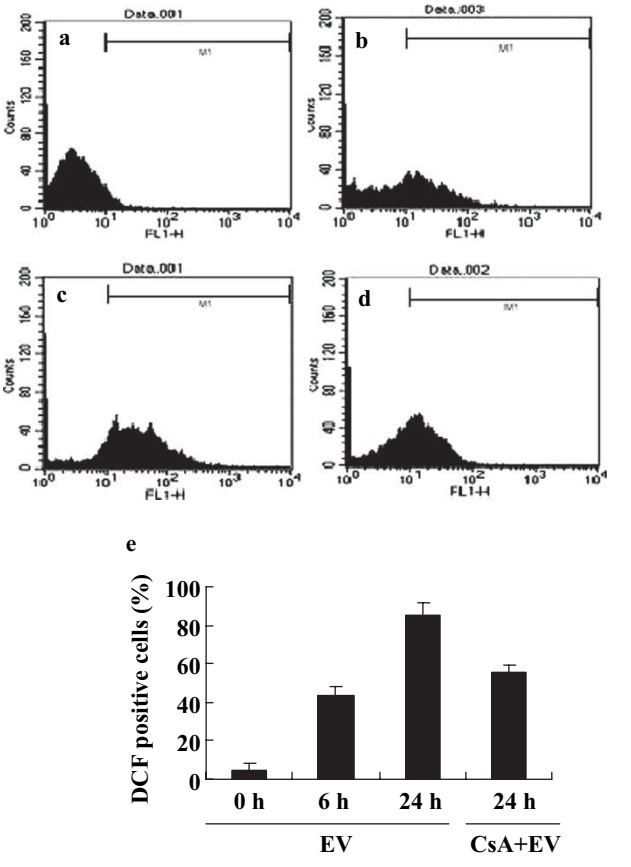

Figure 4. Persistent ROS generation was induced by evodiamine and was blocked by MPT in A375-S2 cells. The cells were cultured in the presence of 15 μM evodiamine for 0 (A), 6 h (B), 24 h (C) or coincubated with 0.2 μM CsA for 24 h (D). DCF, the fluorescent dye product of peroxidized DCF-DA, was measured fluorometrically at 1 h post-treatment. The corresponding linear diagram of the FACScan histograms is expressed in (E). Data from a representative experiment ($n=3$) are shown.

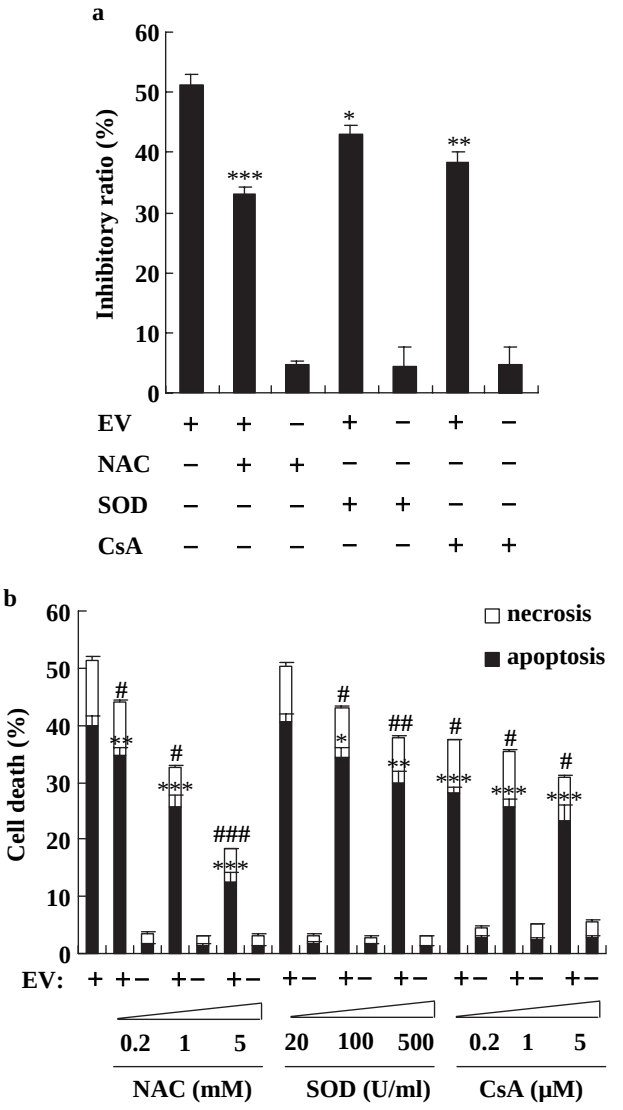

Figure 5. Protective effects of NAC, SOD and CsA on evodiamine-induced cell death. The cells were cultured in the presence or absence of 1 mM NAC, 100 U/ml SOD or 0.2 μM CsA for 1 h prior to the addition of 15 μM evodiamine and then incubated for 24 h. The inhibitory ratio was determined by MTT assay ($n=3$) (A). The cells were pretreated with various doses of NAC, SOD or CsA for 1 h and then incubated with 15 μM evodiamine for 24 h. The cell death rate was measured by LDH activity-based assay (B). Values are expressed as mean ± SD. * $p<0.05$, ** $p<0.01$, *** $p<0.001$ vs the apoptosis percentage in groups treated with evodiamine alone. # $p<0.05$, ## $p<0.01$, ### $p<0.001$ vs the necrosis percentage in groups treated with evodiamine alone.

and enzymatic scavenger SOD, which also functions as an antioxidant by catalysing the conversion of superoxide radicals to hydrogen peroxide, were used to inhibit the intracellular ROS generation. MTT assay displayed that 1 mM NAC markedly reduced the inhibitory ratio from 51.2% for evidiamine alone to 33.0% in the presence of NAC (Figure 5A). Since SOD is poorly cell permeable, although non-physiological concentration at 100 U/ml was applied to treated cells, exogenously delivered SOD could only reduced the inhibitory ratio to 42.9% (Figure 5A). Moreover, MPT inhibitor CsA was applied to block MPT induction. Pre-incubation with 0.2 μM CsA effectively rescued cell death from 51.2% for evodiamine alone to 38.3% in the presence of CsA (Figure 5A).

Cell death may be accomplished by at least two distinct mechanisms, apoptosis and necrosis. To further characterize the mechanisms of evodiamine-induced A375-S2 cell death and to study the effectiveness of inhibitors, the ratios of apoptosis and necrosis in cells were analysed by LDH activity-based assay with or without addition of different doses of inhibitors in evodiamine-treated cells. In the presence of 15 μM evodiamine, the number of apoptotic or necrotic cells was 39.93% or 11.25% at 24 h, respectively, suggesting that necrosis was also triggered by evodiamine in A375-S2 cells, whereas apoptosis was the predominant mechanism responsible for evodiamine-induced cell death within 24 h (Figure 5B). Pre-incubation with 0.2–5 mM NAC, 100–500 U/ml SOD or 0.2–5 μM CsA, the numbers of apoptotic and necrotic cells were both reduced significantly in a dose-dependent manner, among which NAC was the most effective inhibitor (Figure 5B). These results, consistent with the results from Figures 3 and 4, confirmed that ROS production and MPT induction both played important roles in evodiamine-induced A375-S2 cell death.

Evodiamine-stimulated FADD recruitment and procaspase-8 cleavage were significantly blocked by NAC or CsA treatment

The Fas receptor mediated apoptotic signalling is one of the most important extrinsic apoptotic pathways in cells. Binding of Fas to oligomerized FasL activates apoptotic signalling through the death domain that interacts with signalling adaptors including Fas-associated protein with death domain (FADD) to activate caspase-8 following a variety of cellular substrates that lead to cell death [32]. To assess whether Fas-mediated pathway was activated in evodiamine-treated cells, the expressions of FADD and caspase-8 were determined by Western blot analysis. The expression of FADD was markedly elevated and the cleavage of procaspase-8 was obvious after evodiamine administration. Addition of NAC or CsA remarkably inhibited the alterations in FADD and caspase-8; however, SOD could only partially suppress the changes (Figure 6). Therefore, ROS and MPT might be involved in the activation of Fas-mediated apoptotic pathway induced by evodiamine.

Evodiamine-induced Bax translocation, Bcl-2 degradation and SIRT1 inactivation were influenced by NAC or CsA addition

Bax translocation from cytosol to mitochondria was reported to produce some typical manifestations

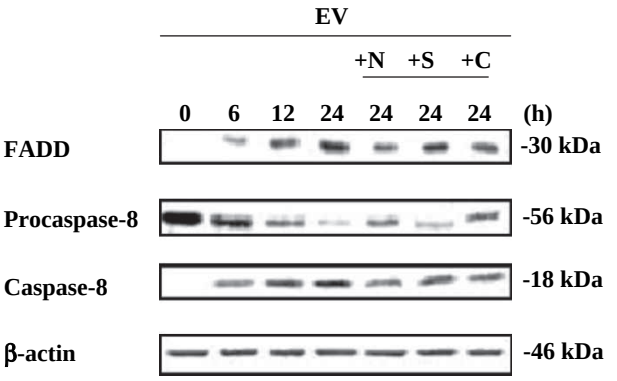

Figure 6. Effects of NAC, SOD and CsA on evodiamine-induced FADD augmentation and procaspase-8 cleaving. The cells were treated with 15 μM evodiamine for the indicated time periods in the presence or absence of 1 mM NAC, 100 U/ml SOD or 0.2 μM CsA, followed by Western blot analysis for detection of FADD and procaspase-8 expressions. β-actin was used as an equal loading control.

of mitochondria-mediated apoptosis, namely release of cytochrome *c* and caspase activation [33]. To investigate the effects of ROS and MPT on the translocation of Bax, the expression of Bax in the cytosol and mitochondria were examined by Western blot analysis. The mitochondrial Bax was significantly increased after evodiamine treatment, but this augmentation was obviously blocked by NAC or CsA employment and was partially suppressed by SOD administration (Figure 7).

Since Bax translocation was down-regulated by either anti-apoptotic protein Bcl-2 or nicotinamide adenine dinucleotide-dependent deacetylase SIRT1, then the levels of Bcl-2 and SIRT1 in evodiamine-treated cells were detected by Western blot analysis.

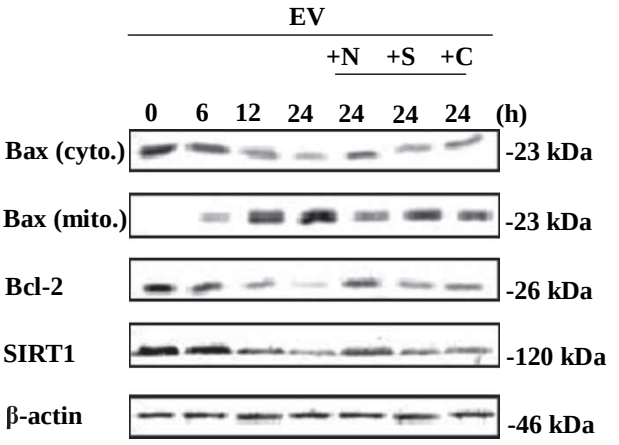

Figure 7. Effects of NAC, SOD and CsA on evodiamine-induced Bax translocation, Bcl-2 degradation and SIRT1 inactivation. The cells were treated with 15 μM evodiamine for the indicated time periods in the presence or absence of 1 mM NAC, 100 U/ml SOD or 0.2 μM CsA, followed by Western blot analysis for detection of Bax, Bcl-2 and SIRT1 expressions both in the cytosol and the mitochondria. β-actin was used as an equal loading control.

Results showed that the expressions of Bcl-2 and SIRT1 were reduced time-dependently by evodiamine treatment and these reductions were notably prevented by NAC or SOD addition, whilst SOD could partially influence them (Figure 7). These events demonstrated that ROS and MPT might participate in the regulation of Bax, Bcl-2 and SIRT1 by evodiamine.

Evodiamine-triggered cytochrome c release was suppressed by NAC, SOD or CsA employment

Since the release of cytochrome *c* from mitochondria to cytosol is a central step of mitochondria regulated apoptotic pathway [34], expressions of cytochrome *c* in the mitochondria and cytosol were separately detected by Western blot analysis. The expression of cytosolic cytochrome *c* was extremely enhanced at 12 h in evodiamine-treated cells; however, this increase was significantly attenuated by co-incubation with NAC or CsA and was partially decreased by SOD addition (Figure 8), revealing that ROS and MPT might contributed to the release of cytochrome *c* induced by evodiamine.

Evodiamine-activated caspase-3 processing was inhibited by NAC, SOD or CsA administration

Caspase-3 is an important protease, activated by cleavage as a step in certain apoptosis-signalling pathways [35]. In this study, the 32 kD caspase-3 proform and the 17 kD active-form from the evodiamine-treated cells were examined by Western blot analysis. A time-dependent cleaving of procaspase-3 was observed in evodiamine treated cells, whereas this processing was notably inhibited by pre-treatment with NAC or CsA and was partially blocked by SOD administration (Figure 9), suggesting that caspase-3 truncation might be enhanced by ROS and MPT in evodiamine treated A375-S2 cells.

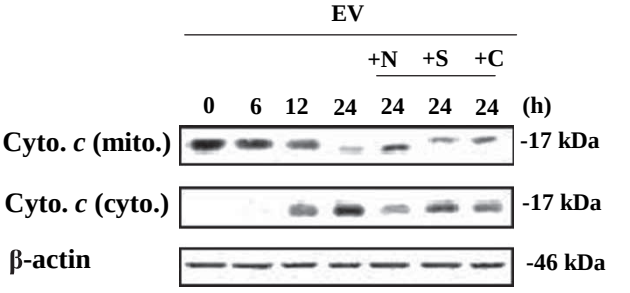

Figure 8. Effects of NAC, SOD and CsA on evodiamine-induced cytochrome *c* release. The cells were treated with 15 μM evodiamine for the indicated time periods in the presence or absence of 1 mM NAC, 100 U/ml SOD or 0.2 μM CsA, followed by Western blot analysis for detection of cytochrome *c* expression both in the mitochondria and the cytosol. β-actin was used as an equal loading control.

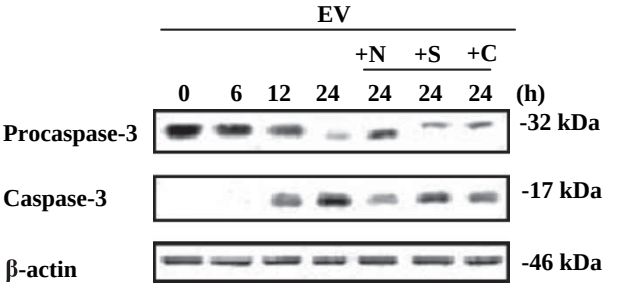

Figure 9. Effects of NAC, SOD and CsA on evodiamine-induced caspase-3 truncation. The cells were treated with 15 μM evodiamine for the indicated time periods in the presence or absence of 1 mM NAC, 100 U/ml SOD or 0.2 μM CsA, followed by Western blot analysis for detection of caspase-3 expression. β-actin was used as an equal loading control.

Discussion

In recent years, it has become clear that mitochondria have significant roles to play not only in routine energy metabolism, but also in cell death. The roles in apoptosis involve a phenomenon called the mitochondrial permeability (MPT), an increase in permeability that seems to be linked to the opening of a channel termed MPT pore which is thought to underlie the loss of mitochondrial membrane potential ($\Delta\Psi$m). Activation of these MPT pores permits the redistribution of molecules across the inner mitochondrial membrane, thus disrupting the $\Delta\Psi$m of this organelle [36]. In this study, an obvious loss of $\Delta\Psi$m was found after 6 h treatment with evodiamine and aggravated until 24 h, suggesting that MPT was induced after incubation with evodiamine for 6 h.

The redox status of intracellular and extracellular compartments is critical in the determination of protein structure, regulation of enzyme activity and control of transcription factor activity and binding [37]. Oxidative stress can evoke many intracellular events including apoptosis. Recent works by a number of groups have demonstrated that ROS can directly modify signalling proteins through different modifications, for example by nitrosylation, carbonylation, disulphide bond formation and glutathionylation. Redox modification of proteins allows for further regulation of cell signalling pathways in response to the cellular environment [38]. Evidences that apoptosis can be induced by ROS are provided by studies in which mediators of apoptosis induce intracellular production of ROS or are inhibited by the addition of antioxidants [39]. It has been further reported that ROS can promote MPT by causing oxidation of thiol groups on the adenine nucleotide translocase (ANT), which is believed to form part of the MPT pore [40]. In this study, a rapid increase in intracellular ROS was observed before $\Delta\Psi$m loss and this depolarization could be reversed by addition of NAC, suggesting a plausible role of ROS in MPT induction. Moreover, the second-time ROS formation at 24 h was found to be blocked by CsA, revealing a positive feed-back role of MPT in ROS production. Additionally, both NAC and CsA were demonstrated to markedly alleviate apoptosis induced by evodiamine. Therefore, two phases of ROS generation existed in treated cells: the first phase corresponded to a combination of basal ROS production and ROS generated as a result of evodiamine induction; the second phase followed by the induction of MPT in mitochondria. This positive feed-back loop of ROS release, or termed ROS induced ROS release (RIRR) which was originally discovered by Zorov [41] in cardiac myocytes, was found for the first time in evodiamine-treated A375-S2 cells and contributed largely to the apoptosis.

It is well known that there are two key pathways which are intrinsic pathway and extrinsic pathway in mediating apoptosis. Mitochondria are major sources of intracellular ROS and are particularly vulnerable to oxidative stress [42]. Bcl-2 family plays a central role in controlling the mitochondrial pathway. It has been suggested that Bcl-2 could prevent apoptosis by regulating the cellular redox potential and act as an antioxidant by increasing the glutathione (GSH) pool and by redistributing GSH to various cellular compartments, thus preventing ROS production, GSH depletion and cellular damage [43]. Bax translocation from cytosol to mitochondria can facilitate cytochrome *c* release from mitochondria either by interacting with the permeability transition pore complex and/or by forming oligomers which act as channels [44]. Bcl-2 can prevent the oligomerization of Bax in the outer mitochondrial membrane, while SIRT1 can deacetylate the DNA repair factor Ku70 to sequester the pro-apoptotic factor Bax away from mitochondria [45]. Our study demonstrated that the first wave of ROS induced by evodiamine contributed largely to the Bax translocation by down-regulation of Bcl-2 and SIRT1 which resulted in MPT induction and final cytochrome *c* release, and then the subsequent onset of MPT facilitated the second wave of ROS which targeted mitochondria again.

Fas is a prototypical 'death receptor' which belongs to the family of tumour necrosis factor receptors (TNFR). Binding of Fas ligand (FasL) to the Fas receptor results in clustering of receptors which then recruit FADD and procaspase-8 to the death-induced signalling complex (DISC) on the cell surface [46]. In this study, both two phases of ROS release induced by evodiamine were observed to participate in the activation of FADD recruitment and caspase-8 processing. It has been reported that Fas possesses abundant thiols in their extracellular domains, which make it susceptible to redox modulation by pro-oxidant agents and processes [47]. We postulated that the ROS induced by evodiamine might influence the downstream effectors by redox modulation of the Fas receptor.

Caspases are cysteine proteases involved in the signalling cascades of programmed cell death in which caspase-3 plays a central role as an 'executioner' enzyme. The intrinsic and extrinsic pathways are known to merge at caspase-3 [48]. Upon activation, procaspase-3 is cleaved at Asp28-Ser29, thereby generating 17 kD active form. From the obtained results, we observed that both ROS and MPT contributed to the caspase-3 truncation induced by evodiamine. This is consistent with the results above that ROS may modulate both mitochondrial and Fas apoptotic pathways, which consequently lead to the same effector caspase-3 to execute the death mission.

In summary, the results presented herein delineate that ROS generation was first induced by evodiamine and was amplified in a positive feed-back manner by induction of MPT in mitochondria. This interesting phenomenon termed RIRR resulted in the constantly elevated ROS level and greatly contributed to the activation of mitochondrial (intrinsic)- and Fas (extrinsic)-signalling pathways in treated cells. ROS facilitated by MPT might serve as second messengers in the process of apoptosis induced by evodiamine in A375-S2 cells.

References

[1] Pascal M, Andrew F, Gerard E. Apoptosis in development. Nature 2000;407:796–801.
[2] Michael OH. The biochemistry of apoptosis. Nature 2000; 407:770–776.
[3] Fulda S, Debatin KM. Extrinsic versus intrinsic apoptosis pathways in anticancer chemotherapy. Oncogene 2006;25: 4798–4811.
[4] Jin Z, El-Deiry WS. Overview of cell death signaling pathways. Cancer Biol Ther 2005;4:139–163.
[5] Budihardjo I, Oliver H, Lutter M, Luo X, Wang X. Biochemical pathways of caspase activation during apoptosis. Annu Rev Cell Dev Biol 1999;15:269–290.
[6] Su CC, Lin JG, Li TM, Chung JG, Yang JS, Ip SW, Lin WC, Chen GW. Curcumin-induced apoptosis of human colon cancer colo 205 cells through the production of ROS, Ca^{2+} and the activation of caspase-3. Anticancer Res 2006;26:4379–4389.
[7] Simbula G, Columbano A, Ledda-Columbano GM, Sanna L, Deidda M, Diana A, Pibiri M. Increased ROS generation and p53 activation in alpha-lipoic acid-induced apoptosis of hepatoma cells. Apoptosis 2007;12:113–123.
[8] Reinecke F, Levanets O, Olivier Y, Louw R, Semete B, Grobler A, Hidalgo J, Smeitink J, Olckers A, Van der Westhuizen FH. Metallothionein isoform 2A expression is inducible and protects against ROS-mediated cell death in rotenone-treated HeLa cells. Biochem J 2006;395:405–415.
[9] Kang YH, Lee E, Choi MK, Ku JL, Kim SH, Park YG, Lim SJ. Role of reactive oxygen species in the induction of apoptosis by alpha-tocopheryl succinate. Int J Cancer 2004;112:385–392.
[10] Klamt F, Dal-Pizzol F, Conte da Frota MLJR, Walz R, Andrades ME, da Silva EG, Brentani RR, Izquierdo I, Fonseca Moreica JC. Imbalance of antioxidant defense in mice lacking cellular prion protein. Free Radic Biol Med 2001;30:1137–1144.
[11] Crack PJ, Taylor JM. Reactive oxygen species and the modulation of stroke. Free Radic Biol Med 2005;38: 1433–1144.
[12] Ermak G, Davies KJ. Calcium and oxidative stress: from cell signaling to cell death. Mol Immunol 2002;38:713–721.
[13] Hunter DR, Haworth RA. The Ca^{2+}-induced membrane transition in mitochondria. I. The protective mechanisms. Arch Biochem Biophys 1979;195:453–459.
[14] Armstrong JS, Whiteman M, Yang H, Jones DP, Sternberg P Jr. Cysteine starvation activates the redox-dependent mitochondrial permeability transition in retinal pigment epithelial cells. Invest Ophthalmol Vis Sci 2004;45:4183–4189.
[15] Amacher DE. Drug-associated mitochondrial toxicity and its detection. Curr Med Chem 2005;12:1829–1839.
[16] Yoshizumi M, Houchi H, Ishimura Y, Hirose M, Kitagawa T, Tsuchiya K, Minakuchi K, Tamaki T. Effect of evodiamine on catecholamine secretion from bovine adrenal medulla. J Med Invest 1997;44:79–82.
[17] Chiou WF, Chou CJ, Shum AY, Chen CF. The vasorelaxant effect of evodiamine in rat isolated mesenteric arteries: mode of action. Eur J Pharmacol 1992;215:277–283.
[18] Kobayashi Y, Nakano Y, Hoshikuma K, Yokoo Y, Kamiya T. The bronchoconstrictive action of evodiamine, an indoloquinazoline alkaloid isolated from the fruits of Evodia rutaecarpa, on guinea-pig isolated bronchus: possible involvement of vanilloid receptors. Planta Med 2000;66:526–530.
[19] Tsai TH, Lee TF, Chen CF, Wang LCH. Thermoregulatory effects of alkaloids isolated from Wu-chu-yu in afebrile and febrile rats. Pharmacol Biochem Be 1995;50:293–298.
[20] Matsuda H, Wu JX, Tanaka T, Iinuma M, Kubo M. Antinociceptive activities of 70% methanol extract of evodiae fructus and its alkaloidal components. Biol Pharm Bull 1997;20:243–248.
[21] Fei XF, Wang BX, Li TJ, Tashino S, Minami M, Xing DJ, Ikejima T. Evodiamine, a constituent of Evodiae Fructus, induces anti-proliferating effects in tumor cells. Cancer Sci 2003;94:92–98.
[22] Zhang Y, Wu LJ, Tashiro S, Onodera S, Ikejima T. Intracellular regulation of evodiamine-induced A375-S2 cell death. Biol Pharm Bull 2003;26:1543–1547.
[23] Jarrett SG, Albon J, Boulton M. The contribution of DNA repair and antioxidants in determining cell type-specific resistance to oxidative stress. Free Radic Res 2006;40: 1155–1165.
[24] Charrier L, Jarry A, Toquet C, Bou-Hanna C, Chedorge M, Denis M, Vallette G, Laboisse CL. Growth phase-dependent expression of ICAD-L/DFF45 modulates the pattern of apoptosis in human colonic cancer cells. Cancer Res 2002;62:2169–2174.
[25] Li D, Wu LJ, Tashiro S, Onodera S, Ikejima T. Oridonin-induced A431 cell apoptosis partially through blockage of the Ras/Raf/ERK signal pathway. J Pharmacol Sci 2007;103: 56–66.
[26] Saris NE, Teplova VV, Odinokova IV, Azarashvily TS. Interference of calmidazolium with measurement of mitochondrial membrane potential using the tetraphenylphosphonium electrode or the fluorescent probe rhodamine 123. Anal Biochem 2004;328:109–112.
[27] Yang ML, Huang TS, Lee Y, Lu FJ. Free radical scavenging properties of sulfinpyrazone. Free Radic Res 2002;36:685–693.
[28] Chen Z, Merta PJ, Lin NH, Tahir SK, Kovar P, Sham HL, Zhang H. A-432411, a novel indolinone compound that disrupts spindle pole formation and inhibits human cancer cell growth. Mol Cancer Ther 2005;4:562–568.
[29] Zhou B, Wu LJ, Li LH, Tashiro S, Onodera S, Uchiumi F, Ikejima T. Silibinin protects against isoproterenol-induced rat cardiac myocyte injury through mitochondrial pathway after up-regulation of SIRT1. J Pharmacol Sci 2006;102:387–395.

[30] Wong YT, Ruan R, Tay FE. Relationship between levels of oxidative DNA damage, lipid peroxidation and mitochondrial membrane potential in young and old F344 rats. Free Radic Res 2006;40:393–402.
[31] Brady NR, Hamacher-Brady A, Westerhoff HV, Gottlieb RA. A wave of reactive oxygen species (ROS)-induced ROS release in a sea of excitable mitochondria. Antioxid Redox Signal 2006;8:1651–1665.
[32] Mitsiades CS, Poulaki V, Fanourakis G, Sozopoulos E, McMillin D, Wen Z, Voutsinas G, Tseleni-Balafouta S, Mitsiades N. Fas signaling in thyroid carcinomas is diverted from apoptosis to proliferation. Clin Cancer Res 2006;12: 3705–3712.
[33] Schinzel A, Kaufmann T, Schuler M, Martinalbo J, Grubb D, Borner C. Conformational control of Bax localization and apoptotic activity by Pro168. J Cell Biol 2004;164:1021–1032.
[34] Garrido C, Galluzzi L, Brunet M, Puig PE, Didelot C, Kroemer G. Mechanisms of cytochrome *c* release from mitochondria. Cell Death Differ 2006;13:1423–1433.
[35] Porter AG, Janicke RU. Emerging roles of caspase-3 in apoptosis. Cell Death Differ 1999;6:99–104.
[36] Ly JD, Grubb DR, Lawen A. The mitochondrial membrane potential (deltapsi(m)) in apoptosis; an update. Apoptosis 2003;8:115–128.
[37] Ghezzi P. Regulation of protein function by glutathionylation. Free Radic Res 2005;39:573–580.
[38] England K, Cotter TG. Direct oxidative modifications of signalling proteins in mammalian cells and their effects on apoptosis. Redox Rep 2005;10:237–245.
[39] Chen WY, Wu CC, Lan YH, Chang FR, Teng CM, Wu YC. Goniothalamin induces cell cycle-specific apoptosis by modulating the redox status in MDA-MB-231 cells. Eur J Pharmacol 2005;522:20–29.
[40] Kanno T, Sato EE, Muranaka S, Fujita H, Fujiwara T, Utsumi T, Inoue M, Utsumi K. Oxidative stress underlies the mechanism for Ca(2+)-induced permeability transition of mitochondria. Free Radic Res 2004;38:27–35.
[41] Zorov DB, Filburn CR, Klotz LO, Zweier JL, Sollott SJ. Reactive oxygen species (ROS)-induced ROS release: a new phenomenon accompanying induction of the mitochondrial permeability transition in cardiac myocytes. J Exp Med 2000;192:1001–1014.
[42] Gao J, Zhu ZR, Ding HQ, Qian Z, Zhu L, Ke Y. Vulnerability of neurons with mitochondrial dysfunction to oxidative stress is associated with down-regulation of thioredoxin. Neurochem Int 2007;50:379–385.
[43] Voehringer DW. BCL-2 and glutathione: alterations in cellular redox state that regulate apoptosis sensitivity. Free Radic Biol Med 1999;27:945–950.
[44] Zhang D, Armstrong JS. Bax and the mitochondrial permeability transition cooperate in the release of cytochrome c during endoplasmic reticulum-stress-induced apoptosis. Cell Death Differ 2007;14:703–715.
[45] Cohen HY, Miller C, Bitterman KJ, Wall NR, Hekking B, Kessler B, Howitz KT, Gorospe M, de Cabo R, Sinclair DA. Calorie restriction promotes mammalian cell survival by inducing the SIRT1 deacetylase. Science 2004;305:390–392.
[46] Lee KH, Feig C, Tchikov V, Schickel R, Hallas C, Schutze S, Peter ME, Chan AC. The role of receptor internalization in CD95 signaling. EMBO J 2006;25:1009–1023.
[47] Dominici S, Pieri L, Paolicchi A, De Tata V, Zunino F, Pompella A. Endogenous oxidative stress induces distinct redox forms of tumor necrosis factor receptor-1 in melanoma cells. Ann NY Acad Sci 2004;1030:62–68.
[48] Basu A, Castle VP, Bouziane M, Bhalla K, Haldar S. Crosstalk between extrinsic and intrinsic cell death pathways in pancreatic cancer: synergistic action of estrogen metabolite and ligands of death receptor family. Cancer Res 2006; 66:4309–4318.